Properties of the 5′→3′ Exonuclease/Ribonuclease H Activity of *Thermus thermophilus* DNA Polymerase

Tatiana Auer, Phoebe A. Landre,‡ and Thomas W. Myers*

Program in Core Research, Roche Molecular Systems, Alameda, California 94501

Received December 15, 1994; Revised Manuscript Received February 3, 1995[⊗]

ABSTRACT: The recombinant 94 kDa *Thermus thermophilus* DNA polymerase (r*Tth* pol) was found to release [^{33}P]UMP when incubated with a RNA·DNA hybrid containing a [^{33}P]UMP-labeled RNA strand. The RNase H activity was optimally active in the presence of low monovalent salt concentrations and when Mn^{2+} was used as the divalent cation activator. RNase H activity also was observed when Mg^{2+} replaced the Mn^{2+}, but to a much lesser extent. A 60 nucleotide long, 5′- or 3′-radiolabeled RNA or DNA oligomer hybridized to a complementary DNA oligomer was used to determine the mode of digestion. The radiolabeled RNA·DNA hybrid or DNA·DNA duplex was incubated with r*Tth* pol using various metal ion conditions and different incubation times. The DNA·DNA duplex showed very little enzymatic cleavage by r*Tth* pol regardless of the Mn^{2+} or Mg^{2+} concentration. However, nearly complete digestion of the RNA·DNA hybrid was observed over a wide Mn^{2+} concentration range, thus demonstrating a preferential degradation of the RNA·DNA hybrid *vs* the DNA·DNA duplex. Time course reactions of the enzymatic digestion of the 3′-labeled RNA·DNA hybrid or DNA·DNA duplex by r*Tth* pol indicated that digestion of the substrates occurred exonucleolytically in the 5′→3′ direction.

Eubacterial single-subunit DNA polymerases, such as *Escherichia coli* DNA polymerase I (*E. coli* pol I),[1] typically share the same structural−functional organization: a 5′→3′ exonuclease, a 3′→5′ exonuclease, and a DNA polymerase. The 5′→3′ exonuclease activity of *E. coli* pol I is known to be responsible for removing DNA lesions during excision repair. This nucleolytic activity can utilize either duplex DNA or RNA·DNA hybrids, cleaving a phosphodiester bond of a base paired region to release either 5′-mononucleotides or oligonucleotides (Lundquist & Olivera, 1982; Kornberg & Baker, 1992). Similar to *E. coli* pol I, *Taq* pol possesses a 5′→3′ exonuclease activity located in the N-terminus of the polypeptide (Lawyer *et al.*, 1989, 1993). Comparisons of amino acid sequences of *E. coli* pol I, *Taq* pol, and r*Tth* pol show a high degree of similarity, suggesting that the enzymatic activities of r*Tth* pol are homologous to those of *Taq* pol and subsequently to *E. coli* pol I (Myers & Gelfand, 1991). The r*Tth* pol is a 94 kDa polypeptide which, like *Taq* pol and *E. coli* of I, possesses 5′→3′ exonuclease activity and DNA polymerase activity. Like *Taq* pol, r*Tth* pol lacks a 3′→5′ exonuclease activity (Myers & Gelfand, 1991; Lawyer *et al.*, 1993).

Partial characterization of the 5′→3′ exonuclease of *Taq* pol indicated that the nucleolytic activity strongly prefers double-stranded over single-stranded DNA and that optimal activity was observed with a nicked DNA substrate (Longley *et al.*, 1990). Further characterization showed that the nuclease activity was enhanced if polymerization occurred concomitantly with the nucleolytic action (Lawyer *et al.*, 1993). The preferred substrate for cleavage is displaced single-stranded DNA, forming a fork-like structure, with hydrolysis occurring at the phosphodiester bond joining the displaced region with the base paired portion of the strand. Therefore, the enzyme is best described as a structure-dependent endonuclease (Holland *et al.*, 1991). Similar substrate preferences for exonucleolytic degradation have been reported for *Thermus flavus* and *Thermus thermophilus* DNA polymerases (Lyamichev *et al.*, 1993), calf 5′→3′ exonuclease (Siegal *et al.*, 1992; Murant *et al.*, 1994), and other mammalian nucleases (Harrington & Lieber, 1994).

The 5′→3′ exonuclease activity of *E. coli* pol I also demonstrates RNase H activity during the removal of RNA from the RNA·DNA hybrids formed during lagging-strand DNA synthesis *in vivo*. A similar function has been suggested for the HSV-1 DNA polymerase, since the enzyme was shown to digest the RNA strand of a RNA·DNA hybrid (Crute & Lehman, 1989). DNA polymerases from *Thermus aquaticus* and *Thermus thermophilus* also have been found to possess a RNase H-type activity (Lyamichev *et al.*, 1993). However, unlike conventional RNase H activities, the RNase H activity described for these two proteins cleaves 5′-overhanging single-stranded RNA at a single site immediately adjacent to a RNA·DNA hybrid. Additionally, the RNase H-type activity of these two proteins was shown to differ, depending upon whether Mg^{2+} or Mn^{2+} was used as the divalent cation activator. The RNase H-type activity of

* Correspondence should be addressed to this author at the Program in Core Research, Roche Molecular Systems, 1145 Atlantic Ave., Alameda, CA 94501. Telephone: (510) 814-2930. FAX: (510) 814-2910.

‡ Present address: Engineering Research Division, Lawrence Livermore National Laboratory, Livermore, CA 94551.

⊗ Abstract published in *Advance ACS Abstracts,* April 1, 1995.

[1] Abbreviations: AMV, avian myeloblastosis virus; DNase, deoxyribonuclease; RNase, ribonuclease; *E. coli* pol I, *Escherichia coli* DNA polymerase I; HSV-1, herpes simplex virus type 1; r*Tth* pol, recombinant *Thermus thermophilus* DNA polymerase; *Taq* pol, *Thermus aquaticus* DNA polymerase; TCA, trichloroacetic acid; bicine, *N,N*-bis(2-hydroxyethyl)glycine; KOAc, potassium acetate; $Mn(OAc)_2$, manganese acetate; dNTP, deoxynucleoside triphosphate; rNMP, ribonucleoside monophosphate; DEAE, diethylaminoethyl; RT, reverse transcription; PCR, polymerase chain reaction; PAGE, polyacrylamide gel electrophoresis; TLC, thin-layer chromatography.

0006-2960/95/0434-4994$09.00/0

the protein from *Thermus aquaticus* functioned with either metal ion, whereas the *Thermus thermophilus* polymerase was active only in the presence of Mg^{2+}.

The characterization of the enzymological properties of r*Tth* pol is of interest because it has become increasingly important in molecular biology applications. The discovery that r*Tth* pol has efficient reverse transcriptase activity in the presence of Mn^{2+} (Myers & Gelfand, 1991) has allowed for high-temperature cDNA synthesis during RT/PCR (Thomas *et al.*, 1992; Young *et al.*, 1993; Schmidt *et al.*, 1993; Mulder *et al.*, 1994), a condition that reduces the secondary structure formation of template RNA, increases the specificity of primer annealing, and allows for the incorporation of the dUTP/uracil-*N*-glycosylase carryover prevention system (Longo *et al.*, 1990). The suggestion that the RNase H activity of the viral reverse transcriptases is detrimental to the production of full-length cDNA (Kotewicz *et al.*, 1988) has prompted us to further characterize the RNase H activity of r*Tth* pol. We have found that the 5′→3′ exonuclease activity of r*Tth* pol preferentially degrades RNA·DNA hybrids *vs* duplex DNA. Additionally, the RNase H activity of r*Tth* pol results either from 5′→3′ exonucleolytic degradation or from structure-specific endonucleolytic action and not from general endonucleolytic cleavage as observed for the viral reverse transcriptases.

EXPERIMENTAL PROCEDURES

Enzymes. r*Tth* pol (2.5 units/μL, 180 fmol/μL) and RNase inhibitor were obtained from Perkin-Elmer. T7 RNA polymerase and RQ1 RNase-free DNase were obtained from Promega. Bovine pancreas DNase-free RNase was from Boehringer Mannheim. All other enzymes were obtained from Gibco BRL.

DNA, Oligonucleotides, and Nucleotides. A 1-kb DNA ladder and a 10-bp DNA ladder were obtained from Gibco BRL. Oligodeoxynucleotides AW116 (5′-CCTGCCCATTCGGAGGAAGAG-3′) and AW117 (5′-TTGGCCACCTTGACGCTGCG-3′) were obtained from Perkin-Elmer. Oligodeoxynucleotides TSA1 (5′-GACTTCATTCTCTGTTTCAGATCCCTTTAG-3′), LIG03 (5′-CCTGCGTCCGACGCAGCGTCAAGGTGGCCAACGACCTGTCCAGGTGAGAAAGAACTGGAG-3′), and MT47 (5′-CTCCAGTTCTTTCTCACCTGGACAGGTCGTTGGCCACCTTGACGCTGCGTCGGACGCAGG-3′), oligoribonucleotide LIG04 (5′-CCUGCGUCCGACGCAGCGUCAAGGUGGCCAACGACCUGUCCAGGUGAGAAAGAACUGGAG-3′), and oligonucleotide MT46 (5′-CTCCAGTTCTTTCTCACCTGGACAGGUCGUTGGCCACCTTGACGCTGCGTCGGACGCAGG-3′ (underlined residues are ribonucleotides) were synthesized on an Applied Biosystems 394 DNA/RNA synthesizer. The 1-kb and 10-bp DNA ladders, AW116, AW117, LIG03, and LIG04 were 5′-labeled with [γ-^{32}P]ATP and T4 polynucleotide kinase. LIG04 was 3′-labeled with [5′-^{32}P]pCp and T4 RNA ligase. LIG03 was 3′-labeled with cordycepin 5′-[α-^{32}P]triphosphate and terminal deoxynucleotidyl transferase. Deoxynucleoside 5′-triphosphates were obtained from Perkin-Elmer. Ribonucleoside 5′-triphosphates were obtained from Pharmacia. Radiolabeled nucleotides were obtained from New England Nuclear.

RNA·DNA Hybrid Preparation. Plasmid pAW109 DNA (Myers & Gelfand, 1991) was purified by CsCl equilibrium sedimentation (Sambrook *et al.*, 1989). The plasmid was digested with *Hin*cII producing a 562-bp fragment containing the promoter for T7 RNA polymerase. Run-off transcription with T7 RNA polymerase was performed in the presence of 500 μM each of ATP, CTP, and GTP and 17.5 μM [α-^{33}P]-UTP (819 Ci/mmol) and generated RNA 527 nucleotides in length. After digestion of the DNA template with RQ1 RNase-free DNase (1 unit/μg of DNA), the RNA was extracted twice with 1 volume of phenol/chloroform/isoamyl alcohol (25:24:1) and once with chloroform/isoamyl alcohol (24:1), and subsequently precipitated 3 times using 3 volumes of ethanol and 2.5 M ammonium acetate to remove unincorporated ribonucleotides. Superscript II RNase H$^-$ reverse transcriptase and primer TSA1, which is complementary to the 3′-terminal 30 nucleotides of the RNA transcript, were used to generate first-strand cDNA. The resulting 527-bp [^{33}P]RNA·DNA hybrid was precipitated with TCA to estimate the amount of unincorporated acid-soluble radionucleotide remaining in the RNA preparation.

RNase H Assays. Reactions (50 μL) containing 140 fmol of [^{33}P]RNA·DNA hybrid were incubated with 130 fmol of r*Tth* pol in the presence of 50 mM bicine-KOH (pH 8.3), 50 mM KOAc (pH 7.5), 8% (w/v) glycerol, and 2.5 mM $Mn(OAc)_2$ for 10 min at 60 °C unless indicated otherwise. Quantitation of RNase H assays was achieved by measuring the amount of acid-soluble radioactivity following TCA precipitation as follows: Carrier nucleic acid (10 μL of salmon sperm DNA at 0.5 mg/mL) and TCA (20 μL of a 10% solution) were added to aliquots (30 μL) of RNase H reactions and incubated on ice for 10 min. After incubation, the sample was centrifuged for 10 min at 13 000 rpm, and 30 μL of the supernatant was added to 1 mL of Ecolume scintillation fluid (ICN). The amount of acid-soluble radionucleotide was quantitated by liquid scintillation spectrometry.

RT and Second-Strand cDNA Synthesis. Reactions (25 μL) containing 250 ng (1.4 pmol) of pAW109 *Hin*cII transcript RNA and 2.7 pmol of primer (AW116 and/or AW117) were incubated in the presence of 1.8 pmol of r*Tth* pol, 50 mM bicine-KOH (pH 8.3), 100 mM KOAc (pH 7.5), 3 mM $Mn(OAc)_2$, 300 μM each of dATP, dCTP, dGTP, and dTTP, and 8% (w/v) glycerol. The primer was either [^{32}P]-AW117 for the RT reaction or AW117 and [^{32}P]AW116 for the combined RT/second-strand cDNA synthesis reaction. The reactions were incubated for 20 min at 60 °C followed by 20 min at 70 °C. Protein was removed by extraction with phenol, and the size distribution of the reaction products was determined by electrophoretic separation on a denaturing polyacrylamide gel. Verification of second-strand cDNA synthesis was made by sequencing the reaction product using [^{32}P]AW117 and the AmpliCycle Sequencing Kit obtained from Perkin-Elmer.

Nuclease Assays. The RNA·DNA hybrid or DNA·DNA duplex was formed by incubating a 3-fold molar excess of unlabeled oligonucleotide to labeled oligonucleotide in 300 mM KOAc for 5 min at 70 °C and allowing the annealing mix to cool to 25 °C over 15 min. Reactions (25 μL) containing 180 fmol of either RNA·DNA hybrid or DNA·DNA duplex were incubated with 180 fmol of r*Tth* pol in 50 mM bicine-KOH (pH 8.3), 100 mM KOAc (pH 7.5), 13% (w/v) glycerol, and 3 mM $Mn(OAc)_2$ for 10 min at 60 °C unless indicated otherwise.

Polyacrylamide Gel Electrophoresis. Denaturing 10% polyacrylamide/7 M urea gel electrophoresis was performed as described (Sambrook *et al.*, 1989). Prior to analysis, a 5× loading buffer containing 60 mM EDTA in formamide was added to the samples, and then they were heated at 95 °C for 5 min. Qualitative analysis was achieved by autoradiography and quantitative analysis by an AMBIS 4000 radioanalytic imager (AMBIS Inc., San Diego, CA).

Thin-Layer Chromatography. RNase H reactions were analyzed by DEAE-cellulose thin-layer chromatography as previously described (Holland *et al.*, 1991).

RESULTS

Initial characterization of the RNase H activity of r*Tth* pol was performed by quantitating the release of acid-soluble [^{33}P]UMP from a [^{33}P]UMP-labeled RNA strand of a 527-bp RNA·DNA hybrid. In order to ensure the integrity and purity of the hybrid substrate, background levels of radiolabeled nucleotide were determined by performing a mock RNase H reaction in the absence of r*Tth* pol. The amount of acid-soluble nucleotide resulting either from unincorporated precursor nucleotides or from metal-ion-catalyzed hydrolysis of single-stranded RNA that was not reverse-transcribed (Brown, 1974; Myers & Gelfand, 1991) was minimal (<5%). Incubation of the [^{33}P]RNA·DNA hybrid with *E. coli* RNase H and subsequent analysis of the reaction products by denaturing polyacrylamide gel electrophoresis demonstrated that the hybrid was completely digestable by the enzyme. However, no digestion products were observed when the hybrid was treated with bovine RNase (data not shown), indicating that single-stranded [^{33}P]UMP-labeled RNA was not present at detectable levels and therefore would not compromise the interpretation of results.

Reaction Conditions. To achieve approximately half of the maximal activity observed in the RNase H assay with r*Tth* pol, the enzyme to substrate ratio had to be nearly 1:1 (140 fmol of substrate:130 fmol of enzyme). Raising the enzyme concentration to 180 fmol (substrate:enzyme ratio 1:1.3) resulted in the degradation of 86% (14 pmol of UMP) of the RNA strand of the RNA·DNA hybrid, whereas lowering the enzyme concentration to 90 fmol (substrate: enzyme ratio 1:0.6) achieved only 10% (1.6 pmol of UMP) degradation of the substrate (Figure 1A). These results suggest that in the absence of DNA polymerization, the blunt-ended RNA·DNA hybrid and/or subsequently formed RNA·DNA hybrid degradation product are not efficiently utilized by the r*Tth* pol.

The RNase H activity associated with r*Tth* pol was found to be optimally active under low monovalent salt conditions. The optimal KOAc concentration was approximately 25–50 mM (data not shown), which is considerably lower than the optimal salt concentration of 75–100 mM for DNA polymerase and reverse transcriptase activity (Myers & Gelfand, 1991). The effect of cosolvents on the RNase H activity of r*Tth* pol also was investigated. The use of DMSO and a neutral polyalcohol such as glycerol or sorbitol was found to increase the efficiency of self-sustained sequence replication (3SR) amplification by enhancing the RNase H activity of AMV reverse transcriptase (Fahy *et al.*, 1991). The RNase H activity of r*Tth* pol was relatively insensitive to the addition of up to 10% sorbitol, glycerol was slightly inhibitory (67% of activity with 10% glyercol), and the reaction was inhibited by DMSO proportional to the concentration (33% of activity with 10% DMSO). Additionally, no stimulatory effect on the RNase H activity of r*Tth* pol was observed with combinations of these cosolvents (data not shown). Subsequent experiments were performed in a final concentration of 10% glycerol (including enzyme contribution), since RT/PCR amplifications performed with r*Tth* pol typically contain 5–15% glycerol.

The RNase H activity of r*Tth* pol has an absolute requirement for a divalent cation. The r*Tth* pol was optimally active using Mn^{2+}, with a range of maximum activity from 1.5 to 2.5 mM $Mn(OAc)_2$ when using bicine-KOH (50 mM, pH 8.3) as the buffer (Figure 1B). Although similar levels of RNase H activity were observed using Tris-HCl (10 mM, pH 8.3), a narrow optimal concentration range of Mn^{2+} was observed for the reaction. When using bicine-KOH as the buffer system in r*Tth* pol catalyzed RT/PCR, a broader [Mn^{2+}] range is achieved (Myers *et al.*, 1994) due to the higher Mn^{2+} binding capacity of bicine (Good *et al.*, 1966). RNase H activity with Mg^{2+} as the divalent cation activator was approximately 10% of the activity observed with Mn^{2+}. The ability of dNTPs to complex Mn^{2+} necessitated the adjustment of the $Mn(OAc)_2$ concentration when dNTPs were added to the reaction. As expected, the addition of 300 μM each of dATP, dCTP, dGTP, and dTTP resulted in a shift of the optimal Mn^{2+} concentration range from 1.5–2.5 to 3.0–4.0 mM $Mn(OAc)_2$.

In the presence of an extendible 3′-hydroxyl group and dNTPs, *E. coli* pol I 5′→3′ exonuclease activity is stimulated 10-fold (Kornberg & Baker, 1992). The increase in nucleolytic activity is observed because a preferred substrate for the exonuclease, i.e., duplex DNA containing a nick, is continually being formed during nick translation synthesis. The addition of dNTPs did not enhance the RNase H activity of r*Tth* pol with the 527-bp RNA·DNA hybrid. This result suggests that the enzyme is not cleaving the RNA endonucleolytically, since such a cleavage would likely result in the formation of an extendible 3′-hydroxyl group. Although these results could be explained if the enzyme were acting endonucleolytically and producing a nonextendible 3′-phosphate, the RNase H activity of r*Tth* pol on this substrate is most likely due solely to the action of the 5′→3′ exonuclease activity in the absence of nick translation synthesis.

The RNase H thermal activity profile of r*Tth* pol showed a maximal activity at 70 °C, with a sharp decline in activity at 75 °C (Figure 1C). The 70 °C temperature optimum determined for RNase H activity is similar to the 60–70 °C optimal temperature observed for DNA polymerase activity on RNA and DNA templates.[2] The dramatic decrease in RNase H activity at 75 °C may be explained in part by the inability of r*Tth* pol to remove the complete RNA strand of the hybrid as a result of strand separation of the RNA·DNA hybrid degradation products. During nucleolytic degradation of the RNA strand of the RNA·DNA hybrid, r*Tth* pol proceeds along the hybrid digesting the RNA. The remainder of the RNA strand, upon reaching the respective strand-separation temperature, would dissociate, thus effectively decreasing the amount of substrate available and concomitantly increasing the amount of acid-precipitable radionucle-

[2] T. W. Myers, unpublished data.

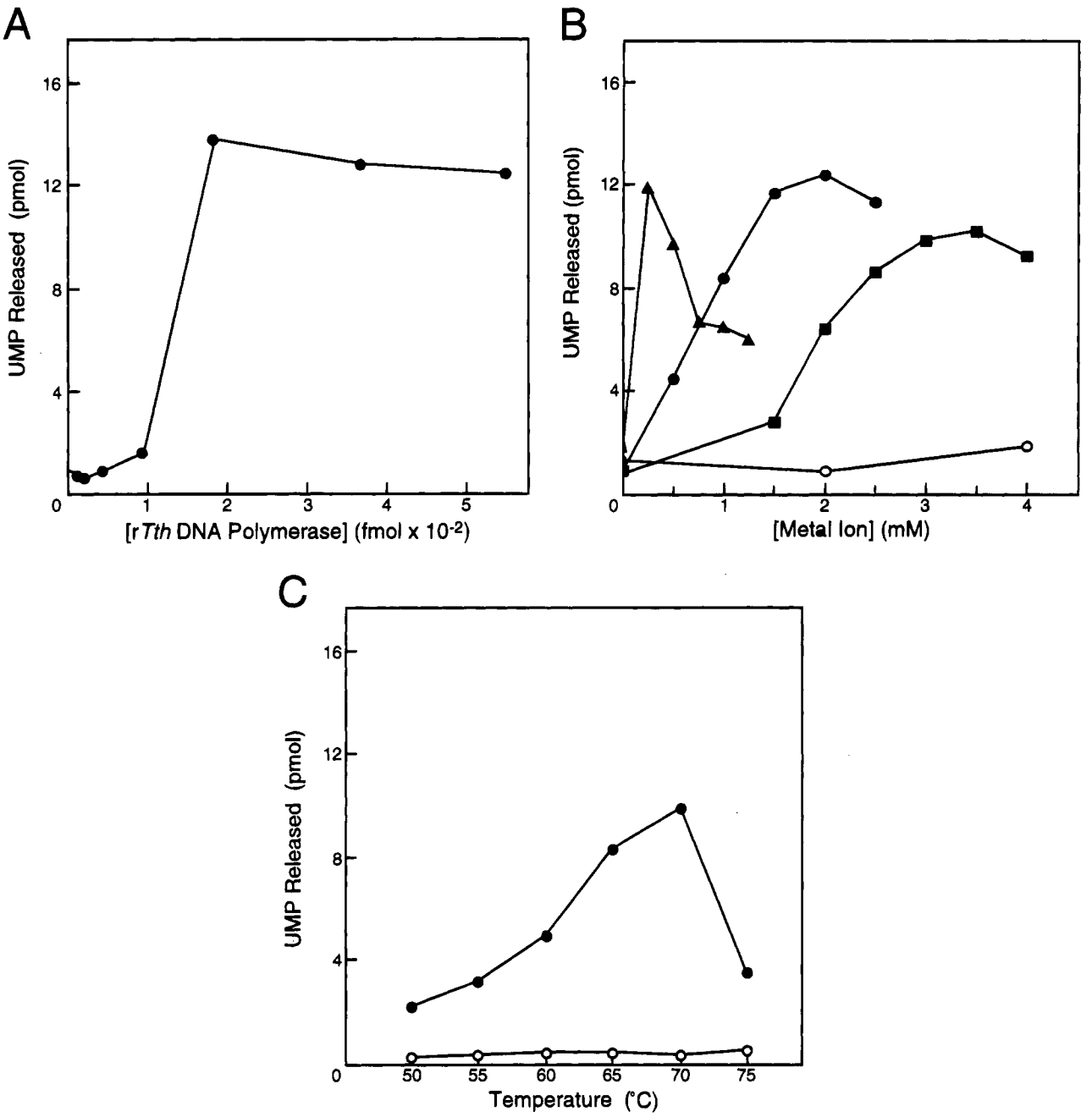

FIGURE 1: RNase H activity associated with r*Tth* pol. RNase H activity was measured by the release of [^{33}P]UMP from a RNA·DNA hybrid as described under Experimental Procedures. (A) RNase H activity with increasing levels of r*Tth* pol using Mn^{2+} as the divalent metal ion. (B) Metal ion requirements for RNase H activity associated with r*Tth* pol. RNase H activity was determined using either $Mn(OAc)_2$ (●) or $MgCl_2$ (○) in the absence of dNTPs or $Mn(OAc)_2$ in the presence of 300 μM each of dATP, dCTP, dGTP, and dTTP (■). Reactions also were performed using 10 mM Tris-HCl (pH 8.3) and 50 mM KCl with $MnCl_2$ (▲) in the absence of dNTPs. (C) Thermal activity profile of r*Tth* pol RNase H activity. RNase H activity was measured at various temperatures as described in the presence (●) or absence (○) of r*Tth* pol using Mn^{2+} as the divalent metal ion.

otide. Additionally, the dissociation of the small RNA·DNA hybrid also would be facilitated by the high concentration of glycerol present in the reaction. Longer reaction times would have resulted in the complete hydrolysis of the dissociated single-stranded RNA by Mn^{2+} catalysis, causing an actual increase in the amount of acid-soluble radionucleotide. Incubation of the RNA·DNA hybrid without enzyme at elevated temperatures did not result in RNA degradation, indicating that the hybrid was stable at elevated temperatures and that "breathing" at the ends of the blunt-ended hybrid and subsequent Mn^{2+}-catalyzed hydrolysis of the single-stranded RNA were not occurring at detectable levels during the 10 min reaction.

Preference of rTth Pol Nuclease Activity for RNA·DNA Hybrid Substrates. To determine the substrate preference of the nuclease activity of r*Tth* pol, oligonucleotides were radiolabeled and hybridized to form blunt-ended [5′-^{32}P]-RNA·DNA hybrids (LIG04/MT47) or [5′-^{32}P]DNA·DNA duplexes (LIG03/MT47) having the analogous sequence. These 60 nucleotide long, double-stranded molecules do not provide an internal free 3′-hydroxyl group to initiate nick translation synthesis. The former substrate also is believed to represent the molecule encountered by the polymerase following the RT step in RT/PCR. During the RT step, a RNA·DNA hybrid is formed, possibly with single-stranded RNA overhangs at both ends due to internal hybridization

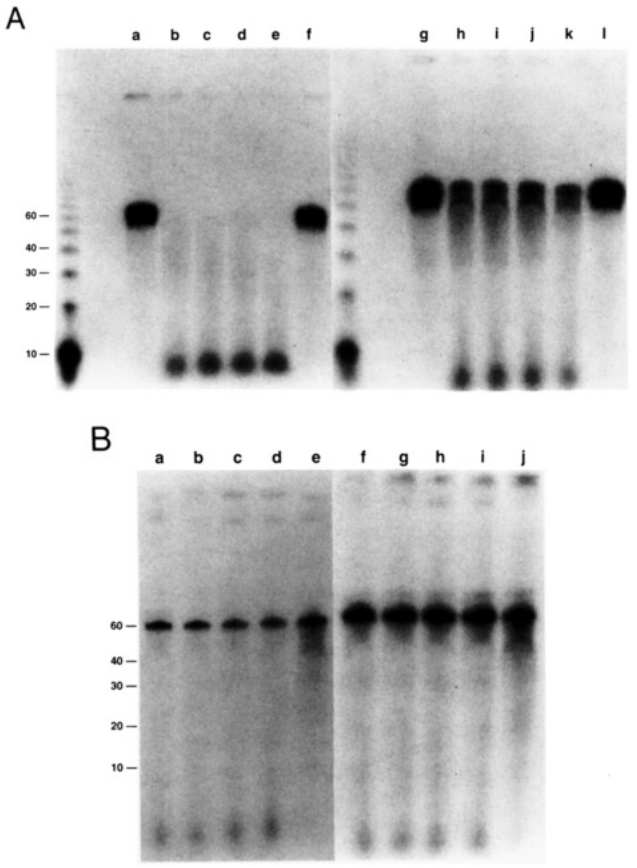

FIGURE 2: Effect of metal ion concentration on nucleolytic degradation of a RNA·DNA hybrid or DNA·DNA duplex. Nuclease activity assays of r*Tth* pol were performed and the reaction products separated by denaturing gel electrophoresis as described under Experimental Procedures, and a 10-bp DNA ladder was used as a size marker. (A) Reactions contained [5′-^{32}P]RNA·DNA hybrid and either 0, 1.5, 3, 5, or 10 mM $Mn(OAc)_2$ (lanes a−e, respectively) or 0, 1.5, 3, 5, or 10 mM $MgCl_2$ (lanes g−k, respectively). Control reactions performed in the absence of r*Tth* pol contained either 10 mM $Mn(OAc)_2$ (lane f) or 10 mM $MgCl_2$ (lane l). (B) Reactions contained [5′-^{32}P]DNA·DNA duplex and either 1.5, 3, 5, or 10 mM $Mn(OAc)_2$ (lanes a−d, respectively) or 1.5, 3, 5, or 10 mM $MgCl_2$ (lanes f−i, respectively). Control reactions performed in the presence of r*Tth* pol were incubated on ice rather than 60 °C and contained either 3 mM $Mn(OAc)_2$ (lane e) or 3 mM $MgCl_2$ (lane j).

and subsequent extension of the RT oligonucleotide on the 3′-end of the RNA and incomplete cDNA synthesis on the 5′-end of the RNA. The single-stranded RNA adjacent to the RNA·DNA hybrid is susceptible to Mn^{2+}-catalyzed hydrolysis at the elevated reaction temperatures; thus, a blunt-ended RNA·DNA heteroduplex will be generated.

Incubation of the 60 nucleotide [5′-^{32}P]RNA·DNA hybrid in the presence of either Mn^{2+} or Mg^{2+} confirmed that a divalent cation activator was required for the r*Tth* pol RNase H activity and that there was a preference for Mn^{2+} as the metal ion (Figure 2A), extending the data monitoring the production of acid-soluble ribonucleotides discussed above (Figure 1B). Analysis of reaction products by denaturing PAGE revealed that the cleavage products were <10 nucleotides in length (Figure 2A, lanes b−e). Further analysis of reaction products by TLC indicated that the nucleolytic digestion of the 5′-labeled hybrid resulted primarily in the release of [^{32}P]CMP, suggesting that digestion occurred exonucleolytically in the 5′→3′ direction (data not shown). Reaction products separated by gel electrophoresis were quantitated on a radioanalytical imager. Greater than 80% of the 5′-terminal ribonucleotide of the RNA·DNA hybrid was cleaved at all Mn^{2+} concentrations evaluated (Figure 2A, lanes b−e). In contrast, only 50−60% of the 5′-terminal ribonucleotide of the RNA·DNA hybrid was digested between 1.5 and 10 mM $MgCl_2$ (Figure 2A, lanes h−k). The apparent increased RNase H activity observed with this substrate in the presence of Mg^{2+} *vs* the results obtained by measuring the release of radiolabeled rNMPs from a RNA·DNA hybrid (Figure 1B) likely reflects the fact that only the 5′-terminal ribonucleotide is labeled and suggests that digestion is occurring in a 5′→3′ direction. The hybrid also was incubated at the respective metal ion concentrations without r*Tth* pol to determine the amount of radiolabel released through metal ion catalyzed hydrolysis of single-stranded RNA resulting either from the "breathing" of the hybrid or from any [5′-^{32}P]oligoribonucleotide that was not annealed to oligodeoxynucleotide. At the highest metal ion concentration evaluated (10 mM), 6.5% of the released label for Mn^{2+} and 4.2% for Mg^{2+} resulted from metal ion catalyzed hydrolysis of RNA at elevated temperatures (Figure 2A, lanes f and l, respectively).

Repeating the metal ion titration with a [5′-^{32}P]DNA·DNA duplex as a substrate, rather than the [5′-^{32}P]RNA·DNA hybrid, demonstrated a preference of the nuclease activity of r*Tth* pol for RNA·DNA hybrids over DNA·DNA duplexes (Figure 2B). Very little digestion of the DNA·DNA duplex was observed when incubated with either Mn^{2+} (Figure 2B, lanes a−d) or Mg^{2+} (Figure 2B, lanes f−i), although more digestion occurred in reactions containing Mn^{2+} *vs* Mg^{2+}.

The RNase H Activity of rTth Pol Is a 5′→3′ Exonuclease. To verify that the digestion of the RNA·DNA hybrid is indeed a result of the 5′→3′ exonuclease activity of r*Tth* pol and not from endonucleolytic cleavage, a RNA 60-mer (LIG04) or a DNA 60-mer (LIG03) of analogous sequence was 3′-radiolabeled and annealed to a complementary DNA 60-mer (MT47). The digestion products of the respective substrates were analyzed at various time points (Figures 3 and 4). Earlier experiments had demonstrated that minimally the 5′-terminus of the available RNA·DNA hybrid substrate molecules was digested by r*Tth* pol after 10 min of incubation at 60 °C (Figure 2A, lane c). Therefore, the time points for the digestion of the 3′-radiolabeled RNA·DNA hybrid were from 0 to 10 min (Figure 3, lanes a−e). Cleavage products of various sizes, ranging from predominantly 25 to 10 nucleotides in length, were formed. As the incubation time increased, the quantity of products from 25 to 10 nucleotides in length increased, whereas the signal intensity for the substrate (60 nucleotides in length) decreased. The absence of any digestion products smaller than 10 nucleotides may be explained by the dissociation of the small RNA fragment from the DNA strand at 60 °C, thus precluding further enzymatic degradation. However, longer reaction times would eventually result in the complete hydrolysis of the dissociated single-stranded RNA by Mn^{2+} catalysis. The appearance of a size distribution of products indicates that the mechanism of cleavage of the 3′-radiolabeled RNA·DNA hybrid by r*Tth* pol occurs exonucleolytically in the 5′→3′ direction in the absence of synthesis.

A time course of a 3′-radiolabeled DNA·DNA duplex also was performed; however, time points from 0 to 60 min (Figure 4) were chosen, due to the extremely low efficiency of substrate utilization observed previously (Figure 2B). The

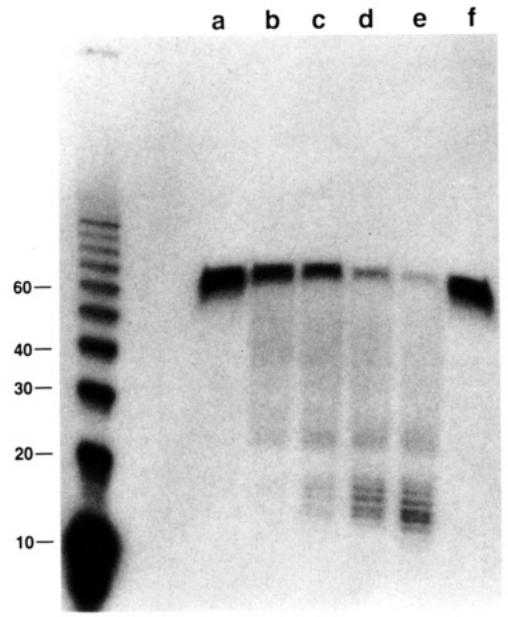

FIGURE 3: Nucleolytic degradation of a [3′-^{32}P]RNA·DNA hybrid as a function of time. Nuclease activity assays of r*Tth* pol were performed and the reaction products separated by denaturing gel electrophoresis as described under Experimental Procedures. Reactions contained 3 mM $Mn(OAc)_2$ and were incubated at 60 °C for either 0, 0.5, 1, 5, or 10 min (lanes a−e, respectively). A control reaction containing 3 mM $Mn(OAc)_2$ was performed for 10 min at 60 °C in the absence of r*Tth* pol (lane f). A 10-bp DNA ladder was used as a size marker.

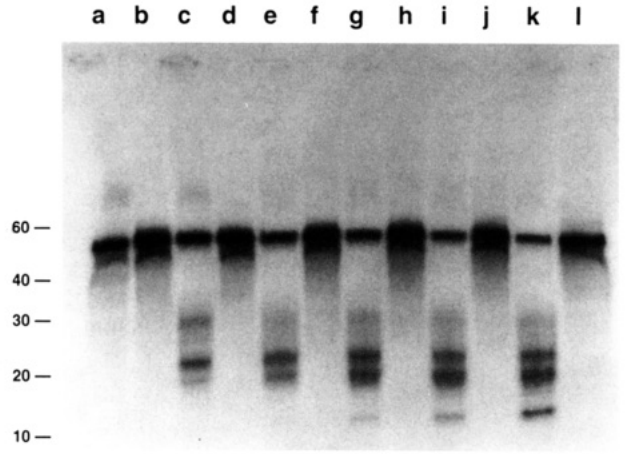

FIGURE 4: Nucleolytic degradation of a [3′-^{32}P]DNA·DNA duplex as a function of time. Nuclease activity assays of r*Tth* pol were performed and the reaction products separated by denaturing gel electrophoresis as described under Experimental Procedures. Reactions contained 3 mM $Mn(OAc)_2$ and were incubated at 60 °C for either 0, 10, 20, 30, 45, or 60 min in the presence (lanes a, c, e, g, i, and k, respectively) or absence of r*Tth* pol (lanes b, d, f, h, j, and l, respectively). A 10-bp DNA ladder was used as a size marker.

size distribution of the cleavage products of the DNA·DNA duplex was similar to that observed for the RNA·DNA hybrid (Figure 3), although considerably less degradation occurred even with a substantially longer incubation time. Additionally, the appearance of larger cleavage products ranging from approximately 30 nucleotides to 20 nucleotides after 10 min of incubation with the DNA·DNA duplex (Figure 4, lane c), compared to the products seen after 10 min with the RNA·DNA hybrid (Figure 3, lane e), further demonstrates that the DNA·DNA duplex is not the preferred substrate of the r*Tth* pol 5′→3′ exonuclease under the conditions investigated. The emergence of digestion products forming a "ladder" was observed with the DNA·DNA duplex after 60 min, whereas a similar distribution of products was seen with the RNA·DNA hybrid after 10 min of incubation. Incubating the DNA·DNA duplex for longer than 30 min with r*Tth* pol resulted in an increase in the amount of cleavage product formed, but the size distribution of the products remained the same. Control reactions (Figure 4, lanes b, d, f, h, j and l) indicated that no nonenzymatic degradation of the DNA·DNA duplex occurred during the extended incubation times.

Further evidence that the RNase H activity is not occurring by endonucleolytic cleavage was obtained by performing experiments as described above, except that the RNA strand of the RNA·DNA hybrid was replaced with an oligonucleotide consisting of RNA flanked on either side by DNA (DNA−RNA−DNA with 23−7−30 nucleotides, respectively). Similar substrates have been used to investigate the kinetic properties of *E. coli* RNase H (Hogrefe *et al.*, 1990). However, unlike the *E. coli* RNase H, endonucleolytic cleavage within the stretch of RNA was not observed, and the size distribution of products was similar to those seen in Figures 2B and 4 for the DNA·DNA duplex (data not shown).

Second-Strand cDNA Synthesis. The reverse transcription of RNA by r*Tth* pol results in a RNA·DNA hybrid, which is a substrate for the RNase H activity of r*Tth* pol. After the degradation of a sufficient amount of RNA from the 5′-terminus to allow hybridization of an oligonucleotide primer complementary to the first-strand cDNA, second-strand cDNA synthesis would be possible with the resultant DNA·DNA duplex being formed in the absence of any high-temperature denaturation step. To determine if indeed second-strand cDNA could be formed without thermal denaturation, we performed reverse transcription with r*Tth* pol using a RNA template 527 nucleotides long (Figure 5). The first-strand cDNA oligonucleotide primer [5′-^{32}P]AW117 binds 168 nucleotides from the 3′-terminus of the RNA. Reverse transcription of the RNA produced an approximately 359-bp RNA·DNA hybrid (Figure 5, lane b). In a separate reaction using unlabeled AW117 for the RT reaction, hybridization of the second-strand cDNA oligonucleotide primer [5′-^{32}P]AW116, which binds 58 nucleotides from the 3′-end of the newly synthesized first-strand cDNA, required that at least 79 nucleotides be removed from the 5′-end of the RNA. Following the removal of the remaining RNA strand by RNase H digestion in the absence of DNA polymerization or by nick translation synthesis, the formation of an approximately 301-bp second-strand cDNA product was observed (Figure 5, lane a). The product was confirmed to be second-strand cDNA by sequence analysis. It is likely that the similar electrophoretic mobility observed for the two complementary DNA strands (359 and 301 nucleotides in length) results from dissimilar base composition, although we cannot rule out the possibility that the first-strand cDNA was not completely full-length either due to premature termination by the polymerase or because the RNA was degraded at the 5′-terminus.

DISCUSSION

The RNase H activity of the viral reverse transcriptases has been suggested to be detrimental to the production of full-length cDNA during reverse transcription due to either competition between cDNA synthesis and RNase H degrada-

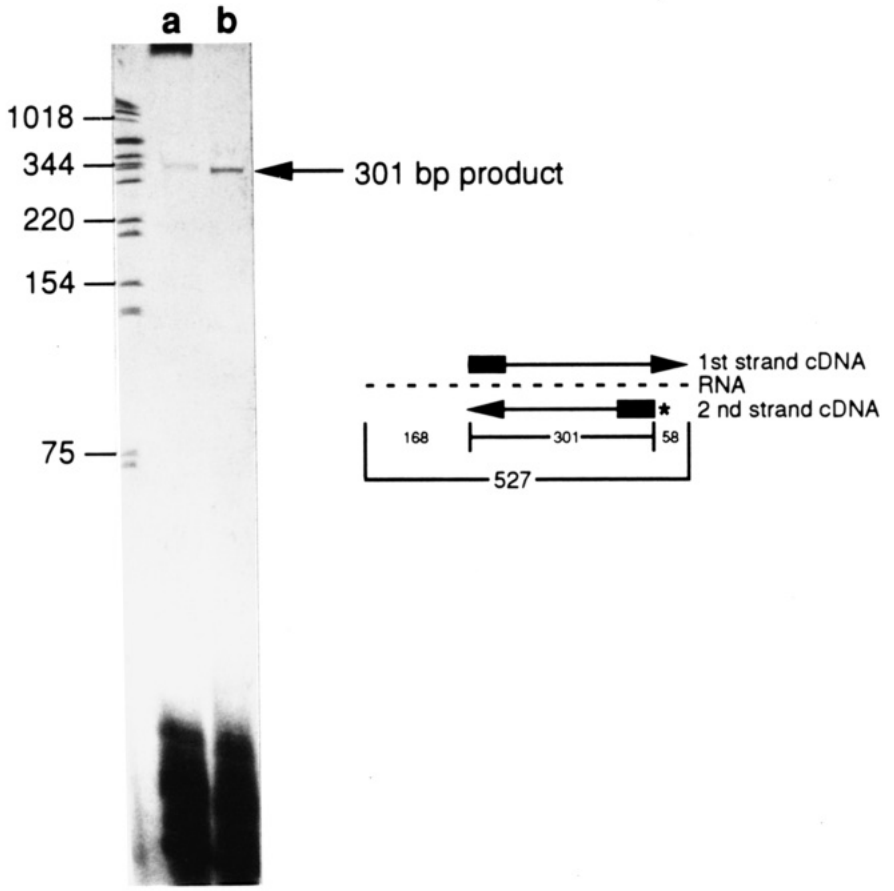

FIGURE 5: Second-strand cDNA synthesis. pAW109 RNA (527 nucleotides) was used as a template for reverse transcription reactions using oligonucleotide primers [5′-^{32}P]AW116 and AW117 to generate radiolabeled second-strand cDNA (lane a) or [5′-^{32}P]AW117 to radiolabel only first-strand cDNA (lane b). Synthesis was performed and the products were separated by denaturing gel electrophoresis as described under Experimental Procedures. A 1-kb DNA ladder was used as a size marker.

tion of the primer-template hybrid or the premature termination of chain elongation during pausing of the polymerase, resulting in cleavage of the RNA template near the 3′-hydroxyl group of the newly synthesized cDNA (Kotewicz *et al.*, 1988). Since r*Tth* pol possesses an inherent 5′→3′ exonuclease activity, the protein also was expected to have RNase H activity similar to *E. coli* pol I. While the nuclease is primarily exonucleolytic in nature, r*Tth* pol, like *Taq* pol, can cleave displaced single-stranded DNA in a structure-dependent endonucleolytic fashion (Holland *et al.*, 1991; Lyamichev *et al.*, 1993). Additionally, a DNA polymerase from *Thermus thermophilus* has been observed to cleave a RNA strand at a single site immediately adjacent to a RNA·DNA hybrid (Lyamichev *et al.*, 1993), a property that would be disastrous during reverse transcription. Although the presence of the 5′→3′ exonuclease activity of r*Tth* pol has not prevented the amplification of DNA targets greater than 40 kb (Cheng *et al.*, 1994), it is unclear whether the presence of a RNase H activity in r*Tth* pol would have any detrimental effect on a RNA template during reverse transcription. The characterization of the enzymatic properties that could affect the ability of r*Tth* pol to reverse transcribe RNA has become increasingly important given the expanded utilization of the protein in RT/PCR amplifications, especially in the area of clinical diagnostics. Therefore, we utilized model substrates to further investigate the RNase H activity of r*Tth* pol and to compare optimal conditions for RNase H activity with those conditions commonly employed during RT/PCR.

The r*Tth* pol RNase H activity has an absolute requirement for a divalent cation. Optimal activity of the r*Tth* pol RNase H activity was observed in the presence of Mn^{2+} *vs* Mg^{2+}. An earlier study using a DNA polymerase from *Thermus thermophilus* and a RNA·DNA hybrid containing 5′-overhanging single-stranded RNA as a substrate observed cleavage of the single-stranded RNA at a single site immediately adjacent to the RNA·DNA hybrid when Mg^{2+} was present, but not when Mn^{2+} was present as the divalent cation (Lyamichev *et al.*, 1993). However, the buffer used for these experiments was Tris-HCl, which allows for a very narrow [Mn^{2+}] range as compared to bicine-KOH (Figure 1B). A titration of Mn^{2+} concentration was not examined in that study, and one explanation for the lack of digestion is that too high of a Mn^{2+} concentration was used, especially in the absence of dNTPs. Additionally, hydrolysis of the 5′-RNA overhang of the substrate would have been expected to reduce the molecule to a blunt-ended RNA·DNA hybrid when incubated with Mn^{2+} at 55 °C for 20 min as described in the study. We were able to detect RNase H activity over a wide range of Mn^{2+} concentrations (1.5−10 mM) when using bicine buffer and a blunt-ended substrate (Figure 2A). A second possibility for the differences observed between our study and Lyamichev *et al.* (1993) is that the *Thermus thermophilus* DNA polymerase used in their experiments was a native protein with a lower molecular mass (92 kDa). If the reduced molecular mass results from a truncation of the protein at the amino terminus, which contains the 5′→3′ exonuclease domain, the RNase H activity of the protein

could be affected. In fact, the supplier of the enzyme utilized in that study states that the enzyme lacks 5′→3′ exonuclease activity. It was also proposed by Lyamichev *et al.* (1993) that the observed inability of *Thermus thermophilus* DNA polymerase to cleave RNA in the presence of Mn^{2+} contributes to the ability of the enzyme to reverse-transcribe RNA, implying that *Taq* pol had nucleolytic activity in the presence of Mn^{2+} and Mg^{2+} and thus would not function as a reverse transcriptase. However, *Taq* pol has been reported to have reverse transcriptase activity in the presence of Mg^{2+} (Jones & Foulkes, 1989; Shaffer *et al.*, 1990; Tse & Forget, 1990) and Mn^{2+}, although at a much lower efficiency than observed for r*Tth* pol in the presence of Mn^{2+} (Myers & Gelfand, 1991).

The RNase H activity observed for r*Tth* pol in this study was found to occur by exonucleolytic digestion of the substrate, unlike the endonucleolytic cleavage observed in retroviral reverse transcriptases or cellular proteins displaying RNase H activity (Krug & Berger, 1989; Wintersberger, 1990). While optimal RNase H activity was observed when Mn^{2+} was used as the divalent metal ion, we saw no metal-dependent difference in the mode of enzymatic cleavage (i.e., endonucleolytic *vs* exonucleolytic), as demonstrated for the RNase H activity of the HIV-1 reverse transcriptase (Zhan *et al.*, 1994). Interestingly, the r*Tth* pol was found to digest RNA·DNA hybrids preferentially over DNA·DNA duplexes in the absence of DNA synthesis. Many studies have investigated the tertiary structure of RNA·DNA hybrids by NMR, Raman spectroscopy, and X-ray crystallography, but the results often have been conflicting (Nakamura *et al.*, 1991). Recent solution studies by NMR suggest that the RNA residues retain their A-form helical structure, while the DNA residues assume an intermediate conformation between A-form and B-form (Salazar *et al.*, 1993; González *et al.*, 1994). It has also been suggested that RNA·DNA hybrids may be more flexible than pure DNA or RNA (González *et al.*, 1994). Whether because of the difference in tertiary structure alone, or in conjuction with Mn^{2+} and/or the elevated temperatures required for r*Tth* pol activity, the enzyme preferentially degrades the RNA strand of a RNA·DNA hybrid. Additionally, regardless of how the protein recognizes the RNA·DNA hybrid, the RNase H activity of r*Tth* pol is attributed to the inherent 5′→3′ exonuclease domain of the protein, since point mutations that eliminate the 5′→3′ exonuclease phenotype also abolish RNase H activity.[3]

A large enzyme to substrate ratio (approximately 1:1) is necessary to ensure hydrolysis of the RNA strand of a RNA·DNA hybrid. This result suggests that in the absence of DNA polymerization, the blunt-ended RNA·DNA hybrid and/or subsequently formed degradation product are not efficiently utilized by the r*Tth* pol, possibly due to a high K_m for these substrates. However, lacking detailed kinetic analyses, we cannot rule out other explanations such as cooperative polymerase binding at high concentrations of r*Tth* pol. Similar high concentrations of r*Tth* pol also were required to achieve predominantly full-length cDNA during reverse transcription (Myers & Gelfand, 1991). Since most applications involving the use of r*Tth* pol for reverse transcription have enzyme concentrations far in excess of specific target template, the newly formed RNA·DNA hybrid substrate for the RNase H activity also would be present at low concentrations and thus would be expected to be degraded.

The RNase H activity of r*Tth* pol could be utilized between the RT step and PCR amplification in a strategy to selectively amplify a RNA target in the presence of duplex DNA containing the analogous target sequence. While the RNase H activity could be supplied by a thermostable RNase H (Itaya & Kondo, 1991; Kanaya & Itaya, 1992), r*Tth* pol can readily reverse transcribe the RNA to form first-strand cDNA, degrade the RNA of the newly formed RNA·DNA hybrid, and perform second-strand cDNA synthesis under the same buffer conditions. The ability to specifically and selectively amplify RNA when genomic DNA of analogous sequence is present becomes very difficult in the absence of introns or presence of pseudogenes. Similar problems also are faced when attempting to distinguish between retroviral RNA and integrated proviral DNA. Several approaches have been developed to differentiate between RNA and DNA of the same sequence (Imboden *et al.*, 1993; Buchman *et al.*, 1993; Tong *et al.*, 1994). However, all of these methodologies have their pitfalls, especially when geared toward clinical diagnostics.

Our strategy for the selective amplification of RNA targets is based simply on the enzymology of a single thermostable protein (r*Tth* pol) and the ability to modulate the strand-separation temperature requirements during the RT/PCR. Following reverse transcription by r*Tth* pol, single-stranded RNA adjacent to the newly formed RNA·DNA hybrid may be present. Negligible single-stranded nuclease activity has been observed when incubating RNA with r*Tth* pol under RT/PCR conditions.[3] However, the RNA would be hydrolyzed in the presence of Mn^{2+} at the elevated temperature. The RNA strand of the blunt-ended RNA·DNA hybrid formed would then be removed by the RNase H activity of r*Tth* pol, thus allowing the second-strand primer to bind to the first-strand cDNA of the hybrid. Synthesis of the second-strand cDNA could then occur by nick translation synthesis or by hydrolysis of the RNA strand prior to synthesis, resulting in a DNA·DNA duplex. The substitution of nucleotide analogues that decrease base stacking interactions and/or hydrogen bonding for standard nucleotides during reverse transcription and subsequent second-strand cDNA synthesis would reduce the strand-separation temperature of the resultant DNA·DNA hybrid. Alteration of the cycling parameters of the subsequent PCR amplification, such that the strand-separation temperature is below that of genomic duplex DNA composed of standard nucleotides, would prevent the genomic DNA from being denatured during amplification. This strategy does however require that the genomic DNA be intact and not contain nicks; otherwise, nick translation synthesis would occur, allowing incorporation of the nucleotide analogues into the genomic DNA with a subsequent decrease in the strand-separation temperature.

ACKNOWLEDGMENT

We gratefully acknowledge T. Martinez and the Roche Molecular Systems DNA Synthesis Group for synthesis of RNA and DNA oligonucleotides and R. Abramson, D. Gelfand, and J. Sninsky for helpful discussions and critical review of the manuscript.

[3] T. Auer, unpublished data.

REFERENCES

Brown, D. M. (1974) in *Basic Principles in Nucleic Acid Chemistry* (Ts'O, P. O. P., Ed.) Vol. II, pp 43−44, Academic Press, New York.

Buchman, G. W., Schuster, D. M., & Rashtchian, A. (1993) *PCR Methods Appl. 3*, 28−31.

Cheng, S., Fockler, C., Barnes, W. M., & Higuchi, R. (1994) *Proc. Natl. Sci. U.S.A. 91*, 5695−5699.

Crute, J. J., & Lehman, I. R. (1989) *J. Biol. Chem. 264*, 19266−19270.

Fahy, E., Kwoh, D. Y., & Gingeras, T. R. (1991) *PCR Methods Appl. 1*, 25−33.

González, C., Stec, W., Kobylanska, A., Hogrefe, R. I., Reynolds, M., & James, T. L. (1994) *Biochemistry 33*, 11062−11072.

Good, N. E., Winget, G. D., Winter, W., Connolly, T. N., Izawa, S., & Singh, R. M. M. (1966) *Biochemistry 5*, 467−477.

Harrington, J. J., & Lieber, M. R. (1994) *EMBO J. 13*, 1235−1246.

Hogrefe, H. H., Hogrefe, R. I., Walder, R. Y., & Walder, J. A. (1990) *J. Biol. Chem. 265*, 5561−5566.

Holland, P. M., Abramson, R. D., Watson, R., & Gelfand, D. H. (1991) *Proc. Natl. Acad. Sci. U.S.A. 88*, 7276−7280.

Imboden, P., Burkart, T., & Schopfer, K. (1993) *PCR Methods Appl. 3*, 23−27.

Itaya, M., & Kondo, K. (1991) *Nucleic Acids Res. 19*, 4443−4449.

Jones, M. D., & Foulkes, N. S. (1989) *Nucleic Acids Res. 17*, 8387−8388.

Kanaya, S., & Itaya, M. (1992) *J. Biol. Chem. 267*, 10184−10192.

Kornberg, A., & Baker, T. A. (1992) in *DNA Replication*, 2nd ed., pp 140−144, W. H. Freeman & Co., New York.

Kotewicz, M. L., Sampson, C. M., D'Alessio, J. M., & Gerard, G. F. (1988) *Nucleic Acids Res. 16*, 265−277.

Krug, M. S., & Berger, S. L. (1989) *Proc. Natl. Acad. Sci. U.S.A. 86*, 3539−3543.

Lawyer, F. C., Stoffel, S., Saiki, R. K., Myambo, K., Drummond, R., & Gelfand, D. H. (1989) *J. Biol. Chem. 264*, 6427−6437.

Lawyer, F. C., Stoffel, S., Saiki, R. K., Sheng-Yung Chang, Landre, P. A., Abramson, R. D., & Gelfand, D. H. (1993) *PCR Methods Appl. 2*, 275−287.

Longley, M. J., Bennett, S. E., & Mosbaugh, D. (1990) *Nucleic Acids Res. 18*, 7317−7322.

Longo, M. C., Berninger, M. S., & Hartley, J. L. (1990) *Gene 93*, 125−128.

Lundquist, R. C., & Olivera, B. M. (1982) *Cell 31*, 53−60.

Lyamichev, V., Brow, M. A. D., & Dahlberg, J. E. (1993) *Science 260*, 778−783.

Mulder, J., McKinney, N., Christopherson, C., Sninsky, J., Greenfield, L., & Kwok, S. (1994) *J. Clin. Microbiol. 32*, 292−300.

Murante, R. S., Huang, L. H., Turchi, J. J., & Bambara, R. A. (1994) *J. Biol. Chem. 269*, 1191−1196.

Myers, T. W., & Gelfand, D. H. (1991) *Biochemistry 30*, 7661−7666.

Myers, T. W., Sigua, C. L., & Gelfand, D. H. (1994) *Miami Short Rep. 4*, 87.

Nakamura, H., Oda, Y., Iwai, S., Inoue, H., Ohtsuka, E., Kanaya, S., Kumura, S., Katsuda, C., Katayanagi, K., Morikawa, K., Miyashiro, H., & Ikehara, M. (1991) *Proc. Natl. Acad. Sci. U.S.A. 88*, 11535−11539.

Salazar, M., Fedoroff, O. Y., Miller, J. M., Ribeiro, S., & Reid, B. R. (1993) *Biochemistry 32*, 4207−4215.

Sambrook, J., Fritsch, E. F., & Maniatis, T. (1989) in *Molecular Cloning: A Laboratory Manual* (Nolan, C., Ed.) 2nd ed., Cold Spring Harbor Laboratory Press, Cold Spring Harbor, NY.

Schmidt, J. V., Carver, L. A., & Bradfield, C. A. (1993) *J. Biol. Chem. 268*, 22203−22209.

Shaffer, A. L., Wojnar, W., & Nelson, W. (1990) *Anal. Biochem. 190*, 292−296.

Siegal, G., Turchi, J. J., Myers, T. W., & Bambara, R. A. (1992) *Proc. Natl. Acad. Sci. U.S.A. 89*, 9377−9381.

Thomas, R. F., Holt, B. D., Schwinn, D. A., & Liggett, S. B. (1992) *Proc. Natl. Acad. Sci. U.S.A. 89*, 4490−4494.

Tong, J., Bendahhou, S., Chen, H., & Agnew, W. S. (1994) *Nucleic Acids Res. 22*, 3253−3254.

Tse, W. T., & Forget, B. G. (1990) *Gene 88*, 293−296.

Wintersberger, U. (1990) *Pharmacol. Ther. 48*, 259−280.

Young, K. K. Y., Resnick, R. M., & Myers, T. W. (1993) *J. Clin. Microbiol. 31*, 882−886.

Zhan, X., Tan, C.-K., Scott, W. A., Mian, M. A., Downey, K. M., & So, A. G. (1994) *Biochemistry 33*, 1366−1372.

BI942883A